Accuracy of tumor motion compensation algorithm from a robotic respiratory tracking system: A simulation study

Yvette Seppenwoolde[a)]
Department of Radiation Oncology, Division of Medical Physics, ErasmusMC, Rotterdam, The Netherlands

Ross I. Berbeco
Brigham and Women's Hospital and Harvard Medical School, Boston, Massachusetts 02115

Seiko Nishioka
Department of Radiation Oncology, NTT East Japan Sapporo Hospital, Sapporo, Japan

Hiroki Shirato
Department of Radiation Medicine, Hokkaido University School of Medicine, Sapporo, Japan

Ben Heijmen
Department of Radiation Oncology, Division of Medical Physics, ErasmusMC, Rotterdam, The Netherlands

(Received 17 October 2006; revised 19 April 2007; accepted for publication 19 April 2007; published 13 June 2007)

The Synchrony™ Respiratory Tracking System (RTS) is a treatment option of the CyberKnife robotic treatment device to irradiate extra-cranial tumors that move due to respiration. Advantages of RTS are that patients can breath normally and that there is no loss of linac duty cycle such as with gated therapy. Tracking is based on a measured correspondence model (linear or polynomial) between internal tumor motion and external (chest/abdominal) marker motion. The radiation beam follows the tumor movement via the continuously measured external marker motion. To establish the correspondence model at the start of treatment, the 3D internal tumor position is determined at 15 discrete time points by automatic detection of implanted gold fiducials in two orthogonal x-ray images; simultaneously, the positions of the external markers are measured. During the treatment, the relationship between internal and external marker positions is continuously accounted for and is regularly checked and updated. Here we use computer simulations based on continuously and simultaneously recorded internal and external marker positions to investigate the effectiveness of tumor tracking by the RTS. The Cyberknife does not allow continuous acquisition of x-ray images to follow the moving internal markers (typical imaging frequency is once per minute). Therefore, for the simulations, we have used data for eight lung cancer patients treated with respiratory gating. All of these patients had simultaneous and continuous recordings of *both* internal tumor motion and external abdominal motion. The available continuous relationship between internal and external markers for these patients allowed investigation of the consequences of the lower acquisition frequency of the RTS. With the use of the RTS, simulated treatment errors due to breathing motion were reduced largely and consistently over treatment time for all studied patients. A considerable part of the maximum reduction in treatment error could already be reached with a simple linear model. In case of hysteresis, a polynomial model added some extra reduction. More frequent updating of the correspondence model resulted in slightly smaller errors only for the few recordings with a time trend that was fast, relative to the current x-ray update frequency. In general, the simulations suggest that the applied combined use of internal and external markers allow the robot to accurately follow tumor motion even in the case of irregularities in breathing patterns. © *2007 American Association of Physicists in Medicine*. [DOI: 10.1118/1.2739811]

Key words: image guided radiotherapy, respiratory tumor motion, cyberknife, lung cancer

I. INTRODUCTION

The Synchrony™ Respiratory Tracking System (RTS) is a subsystem of the CyberKnife robotic treatment device (Accuray, Inc., Sunnyvale, CA[1–3]) to irradiate extra-cranial tumors that move due to respiration.[4] The advantage of the RTS is that patients can breath normally throughout treatment while the CyberKnife robot actively compensates for breathing motion.

Tumor tracking is based on a fitted curve through a discrete set of points, each consisting of a measured internal tumor position, and a simultaneously measured external (chest/abdominal) marker position, designated correspondence model, or prediction model. The treatment beam follows the *internal* movement via continuously measured *external* movement, a conversion to the corresponding internal movement using the correspondence model, and a compensation using the robot.

TABLE I. Patient information. Patient 5 was treated twice at the same site, with two months between treatments.

Patient	Gender	Age	Tumor pathology	Number of implanted markers	Tumor site[a]	Prescribed dose	Fractions
1	F	47	Adenocarcinoma	4	R S7	N/A	1
2	F	70	Adenocarcinoma	3	L S6	N/A	1
3	F	71	Adenocarcinoma	2	R S5	N/A	1
4	F	47	Adenocarcinoma	3	R S4	48	8
5	M	81	Squamous cell carcinoma	3	R S6b	48	4
5						40	8
6	M	61	Small cell lung cancer	3	R S10	40	8
7	M	68	Squamous cell carcinoma	3	R S6	48	4
8	M	85	Adenocarcinoma	3	R S8	48	4

[a]Tumor site is indicated using common anatomical notation for lung segmentation: S1-3 is upper lobe, S4-5 is middle lobe, S6-10 is lower lobe.

Before treatment starts, the 3D internal tumor position is determined at discrete time points by automatically detecting implanted gold fiducials in orthogonal x-ray images. The external signal is continuously measured using optical LEDs that can be fitted on a tight Velcro vest that the patient is wearing during the treatment. The correspondence model is a linear or polynomial fit between 3D target positions and scalar marker positions (r). During treatment, the model is checked and updated regularly by acquiring additional x-ray images. The update procedure is based on the first-in, first-out principle, i.e., after acquisition of a new pair of x-ray images, a new correspondence model is built using these images and all images used to establish the current correspondence model, except the pair that was acquired first.

Compared to other systems like gating[5–7] or active breathing control,[8,9] another advantage of this system is, like the real-time tumor tracking system,[10,11] that the localization of the internal tumor position is very precise and does not depend on patient positioning errors. During the treatment the relation between internal and external motion is always accounted for and is regularly checked and updated. Furthermore, the duty cycle is, in general, 100%.

However, as for all other breathing compensation/gating methods, irregular tumor motion may adversely impact precision. Therefore, in the current paper, we have tried to answer the following questions:

- How do the applied prediction models depend on the number of acquired x-ray images and the time between subsequent x-ray images?
- Can the RTS follow changes and irregularities in breathing patterns in the time interval between subsequent x-ray acquisitions?
- What if phase differences exist/change during treatment?

II. METHODS AND MATERIALS

A. Patients

To minimize the imaging dose received by the patient in a CyberKnife treatment using RTS, the frequency of update x-ray image acquisition is typically once per 1 to 5 min. The tumor motion is not measured in the intervals between update x-ray images. Therefore, the Cyberknife log files do not contain data to assess the tracking accuracy *within* these intervals and to simulate effects of more frequent updating of the correspondence model. For these reasons we used synchronized recordings of both *internal* tumor motion and *external* abdominal motion of eight lung cancer patients (with estimated tumor motion greater than 1 cm peak-to-peak), treated with real-time-tumor radiotherapy from the study of Berbeco *et al.*,[12] to investigate the breathing compensation method of the RTS. The average length of the 117 recordings was 82 s (range 20 to 250 s) of which 46 lasted longer than 100 s. The patients who were suitable for (and treated by) amplitude-based threshold gating, did not exhibit excess baseline shifts.

These recordings were made at the Radiation Oncology Clinic at the Nippon Telegraph and Telephone Corporation (NTT) Hospital in Sapporo, Japan, that is equipped with a Mitsubishi RTRT system.[11] Patients with abdominal and thoracic tumors treated with this system typically have two to four 1.5 mm diam gold ball bearings implanted in or near the tumor.[13] These markers are tracked in real-time with diagnostic x-ray fluoroscopy and the treatment beam is turned on when a marker is within a predetermined 3D window.[11]

The system at the NTT Hospital differs from the usual RTRT system[10,14] in that there are only two pairs of x-ray tubes and imagers rather than four. Therefore, at some gantry angles, one of the x-ray views may be blocked. To facilitate gating at these angles, an external surrogate gating system was installed and integrated with the RTRT system by Mitsubishi. The AZ-733V external respiratory gating system (Anzai Medical, Tokyo, Japan) uses a laser to monitor the movement of the patient's abdominal surface. For the purposes of this study, the external surface was also monitored when neither of the x-ray views was obscured. The signal from the surface monitor is synchronized with the signal from the fluoroscopic unit so that the log files contain both the three-dimensional tumor position and the external surface position at every time point. The rate of data acquisition for this entire system was 30 frames/s.

The details of each patient are given in Table I.[12] Patients 1–3 have data for one single day because they were brought to the NTT Hospital for the specific purpose of acquiring data for the study of Berbeco *et al.*[12] Patients 4–8 were treated with 40–48 Gy in 4–8 fractions. Patient 5 was treated twice, two months apart. Since the same site was treated and no isocenter shift was made, we used both sets of data in the evaluation, under the same patient name. To give an idea of the variety in breathing patterns, in Fig. 1 tumor positions are plotted as a function of the external signal for one breathing cycle of each patient.

B. Correspondence models

We used the RTRT logged recordings to simulate Cyberknife/RTS treatments with a program written in Matlab® (Mathworks), containing the same mathematics as used for the prediction models in the Synchrony RTS. Additionally, the measured external signal could be shifted in time artificially to simulate the effect of large phase differences. An example of a recording is shown in Fig. 2(a).

By building correspondence models based from the external signal and "snap-shots" of the true internal tumor position during the intial part of each recording (mimicking a Cyberknife treatment), the predicted tumor position during the remainder of the recording could be checked against the true tumor position, using the measured data from the RTRT system as a "gold standard."

For establishing a correspondence model, two options are provided in the RTS:

(1) A linear model, that is simply a linear fit between target positions (3D) and scalar external marker positions (r),

$$\begin{pmatrix} x \\ y \\ z \end{pmatrix}_{\text{Target}} = \begin{pmatrix} A_x \\ A_y \\ A_z \end{pmatrix} r + \begin{pmatrix} B_x \\ B_y \\ B_z \end{pmatrix}.$$

Coefficients (A,B) are found by least-squares fitting to image/marker data-points (Fig. 3).

(2) A polynomial model with two fitted second-order polynomials, one through the image/marker data-points that are determined to be in the inhale phase of the breathing cycle, and one that is determined for the exhale phase,

$$\begin{pmatrix} x \\ y \\ z \end{pmatrix}^{\text{TLS}}_{\text{Target}} = \begin{pmatrix} A_x \\ A_y \\ A_z \end{pmatrix} r^2 + \begin{pmatrix} B_x \\ B_y \\ B_z \end{pmatrix} r + \begin{pmatrix} C_x \\ C_y \\ C_z \end{pmatrix}.$$

An example is shown in Fig. 4.

To determine which model is most appropriate for a particular patient, the following protocol is applied by the RTS and simulated in this study. As new x-rays are introduced into the data set, all possible model types (i.e., linear, curvilinear, and bi-curvilinear) are evaluated to find the optimal one. For each model type, a least-square fit is applied to find the parameters of the model. Then each model type's index of merit is calculated. The index of merit is a slightly modified form of the standard error and is defined as

$$e_m = \sqrt{\frac{\Sigma e_i^2}{n-m}}$$

where e_i: difference between model and ith model point, n: number of points in the model dataset, and m: number of parameters to uniquely define the model (e.g., linear: 2, second order: 3).

The final selection of which model will be used is based on a weighted comparison of these indices of merit. These weights are predetermined and are designed to favor simpler model types (i.e., a linear model has about twice the weight of a polynomial model). It can occur that, for example, for the AP and LR directions the tumor position is predicted by a linear model, while for the CC direction a polynomial model is applied.

If in the course of treatment the LED motion range exceeds the range captured during building of the correspondence model, the quadratic fits are weighted back towards the single linear fit; this prevents the danger of large extrapolation errors that might be possible with a quadratic fit (Fig. 4).

C. Time series

For building a correspondence model, the number of simulated x-ray images and the time between acquisition of x-ray images could be varied. A random number generator was used to generate a number of different patterns of x-ray sequences with similar properties, to be able to determine the variance/stability for each simulation. Three basic patterns were compared:

Pattern 1: Fifteen simulated x-ray images taken at 0.5 s time intervals to ensure that one (or more) breathing cycles were covered homogeneously.

Pattern 2: Using a random generator, 15 simulated x-ray images were taken randomly throughout the same period of time and with, *on average*, 0.5 s time interval.

Pattern CK: Fifteen simulated x-ray images were taken randomly throughout a longer period of time and with, *on average*, two s time interval. This sequence most closely resembles a real Cyberknife treatment.

For time series that were longer than 2 min, updated x-ray images were simulated with variable time intervals (5, 15, and 25 s, or 15 x-ray images with one second delay halfway through the recording to study the effect of completely updating the model). Compared to the clinical situation, the update frequency is higher in the simulations because the length of the time series is too short to simulate 1 to 5 min intervals). Furthermore, the number of simulated x-ray images in the model varied from 3 to 15 to investigate the stability of the correspondence models (always 15 for real treatments).

We evaluated the accuracy of the RTS by determining the average and the 95th percentile of the 3D residual motion over each fraction. The 3D residual error was calculated by determining the 3D distance between the predicted tumor position and the actual tumor position. Furthermore, we split

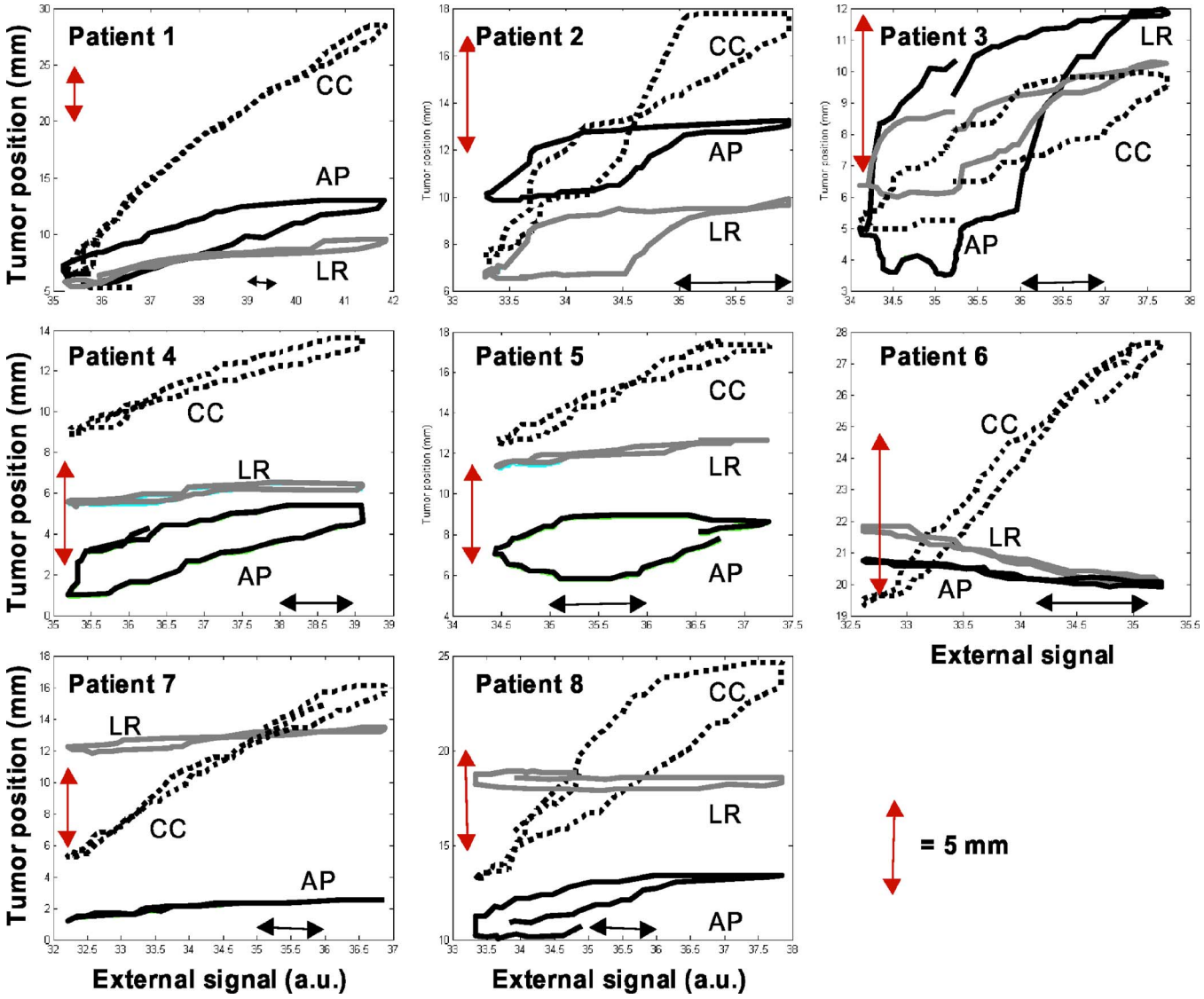

FIG. 1. Examples of the trajectories of one breathing cycle for each patient. Note the complex shapes of the trajectories for patient 2,3,5, and 8 and be aware of the different scales on the axes (the arrows indicate 5 mm).

up the error calculations in three directions and calculated the mean and standard deviation (systematic and random error, respectively).

For the non-compensated treatment, the average tumor position throughout the first 10 s of the fraction was set as the "predicted" tumor position. This is more or less a best case scenario because in noncompensated treatments the average tumor position is not known *a priori* and usually set-up errors (in the order of 3–5 mm) will be present that reduce the accuracy of the non-compensated treatment additionally. For treatments with the Synchrony™ RTS, set-up errors are virtually absent (<1 mm) because of the imaging technique.

III. RESULTS

With the use of the Synchrony™ RTS and pattern 1 as time series (Sec. II C), 3D treatment errors due to breathing motion were reduced in all eight patients (Fig. 5). Between patients and also within patients, a certain variation in the results was observed. A large part of the maximal reduction in treatment error (which was obtained using the polynomial model in most patients) could already be reached with a simple linear model. For patients with hysteresis (internal-internal or internal-external, patients 4 and 5), the polynomial model reduced the residual error compared to the linear model. The reduction in treatment error following the clinical protocol did not always lead to the combination of linear and polynomial models that resulted in the smallest possible residual error. This is due to the applied weighting for model selection (Sec. II B).

The residual treatment error was larger for fractions with more motion and also for patients with more tumor motion. In the course of treatment (over subsequent beams and days), the treatment error did not show a time trend.

In Fig. 2(a), an example of a time registration of the external signal and the x, y, and z coordinates (mm) of the tumor position is shown. The breathing pattern of this patient

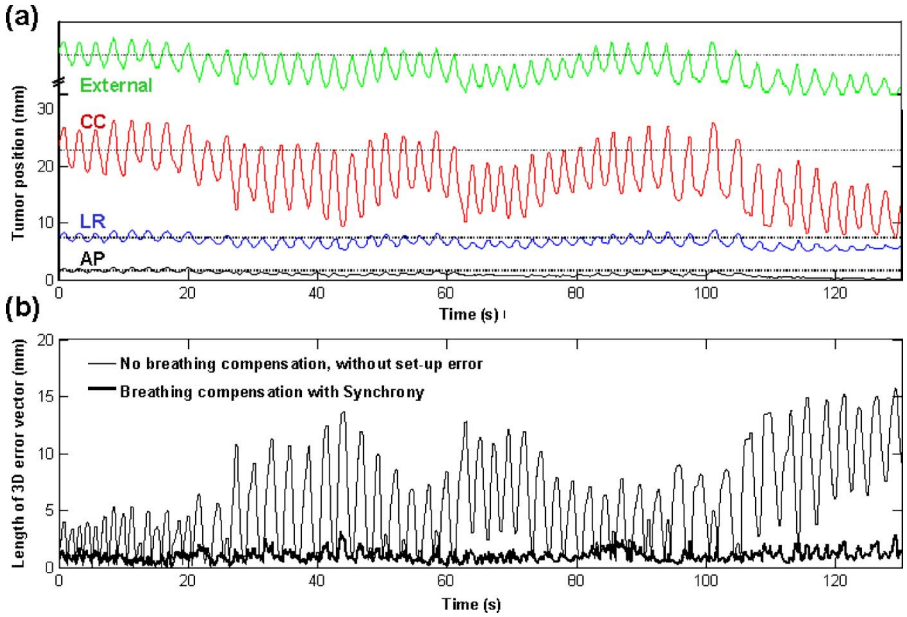

FIG. 2. (a) Example of a time registration of the external signal [expressed in arbitrary units (a.u.)] and x, y, and z co-ordinates (mm) of the tumor position during a >2 min registration recorded from the RTRT system. The straight dotted lines represent the average tumor position calculated over the first 10 s of the recording (this position is assumed to be the "predicted" tumor position for non-compensated simulation). The breathing pattern of this patient is irregular in amplitude, frequency, and baseline. (b) 3D treatment error calculated for a simulated non-compensated treatment and for a Cyberknife treatment with simulated Synchrony™ RTS breathing compensation (linear correspondence model). For the non-compensated treatment, the error increases as the treatment progresses, while the Cyberknife robot is able to follow the tumor with a high accuracy.

was irregular in amplitude, frequency, and baseline. The plot of the 3D treatment error [Fig. 2(b)] shows that for a non-compensated treatment, the error increases as the treatment progresses, while the Cyberknife robot combined with Synchrony™ RTS is able to follow the tumor with high accuracy, even without updating the model in the shown time period.

The correspondence models for this example are shown in Fig. 3. In this case, a linear model was accurate enough to predict the tumor position based on the information obtained from 15 x-ray images in the first 15 s of the simulated treatment.

In Fig. 4, a similar plot is depicted for a patient with hysteresis between internal and external signals; the correspondence model can be approximated with a linear function and this will reduce the treatment error somewhat but, especially in the z-direction (AP), the linear model is not very accurate. With the correspondence model that is based on two polynomial functions, the residual error became smaller. This model is especially appropriate in cases of internal hysteresis or if phase shifts between the internal and external motion are present. In Fig. 6(a) the 3D effect of the polynomial model is compared to the non-compensated case.

The theoretical minimum number of model points (x-ray image pairs) to define a linear model is two. However, the system requires the user to take at least one additional data point before continuing (i.e., three are required). For the polynomial model the theoretical minimum is six model points (and, therefore, the system requires a minimum of eight, four in each phase). However, making a robust model requires an even spread of the data points along different phases of respiration. The system checks that the model points are distributed across a significant proportion of the motion range and prevents treatment starting until they do so. Depending on patients breathing pattern and distribution of model points, 8–12 model points are usually enough to construct a robust polynomial model.

In Fig. 7, the effect of the number of x-ray images in each model is plotted for two patients with irregular breathing patterns and hysteresis. As the number of x-ray images increase, both the residual 3D-treatment errors are reduced, as well as the variability in the results (each simulation was repeated seven times with different x-ray times to ensure good coverage over the range of possibilities (random generator, Sec. II C. For the linear model, six or more x-ray images were enough to ensure consistent results with little variability. For the polynomial model, more than ten x-ray images resulted in more or less consistent results, but the variability only reduced to the level of the linear model for 15 or more images. For patients with a high internal-external correlation, fewer images are necessary to model the motion consistently. These results prove that the settings of Synchrony™ RTS are well-chosen.

To determine the effect of the RTS for the AP, LR, and CC directions separately, we split up the error calculations in three directions (Fig. 8). As expected, breathing motion was largest in the CC direction in most patients and the reduction in treatment error was largest in this direction. For patients 4, 6, and 7, the motion in the other directions was very small and correction for this motion was not really necessary.

In Fig. 9, all data is summarized in two histograms of the mean and the 95th percentage of the 3D treatment error for

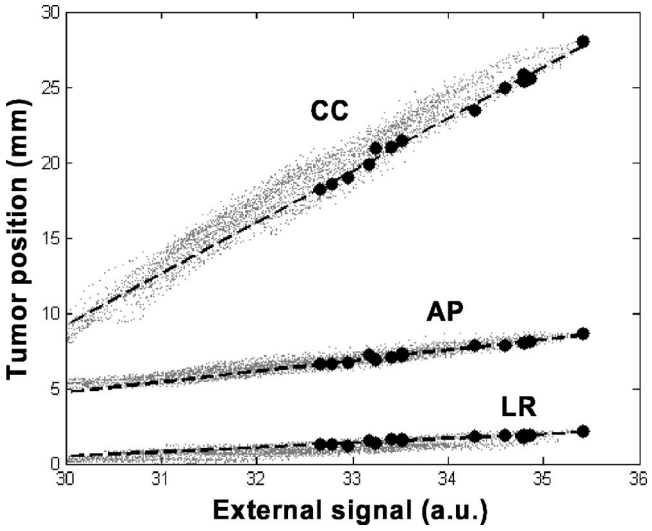

FIG. 3. Linear correspondence model for the same patient as in Fig. 2 (dashed lines) based on 15 simulated x-ray images (solid circles), taken in the first 15 s of the treatment (two or three breathing cycles). The actual tumor position during the treatment as a function of the external signal is plotted as an illustration in the background (tiny dots).

all patients. For the breathing compensated treatments, the residual error was largely reduced and more normally distributed.

A. Gradual changes in correspondence model

The results presented so far show that 15 x-ray images to establish the correspondence model at the start of the treatment are enough to reliably predict the internal tumor position from an external signal for the studied time range (20 to 250 s). But we also observed that, in a few cases, a time trend was present within a single fraction; the correspondence model should have changed gradually over time for a proper prediction. For those cases, the model update function was implemented in Synchrony™ RTS: during treatment, the model is updated regularly by acquiring additional x-ray images and rebuilding the correspondence model based on the first-in, first-out principle (Sec. I). To quantify the effect of updating the model during treatment, we performed simulations using the longest available recordings (140–250 s). At different regular time intervals, an extra x-ray was simulated (every 5, 15, 20 seconds) or a complete update of the model (15 x-ray images at 0.5 s distance) halfway through the recording. The correspondence model was updated accordingly (note that the x-ray update frequency in this experiment was much higher than during a typical Cyberknife treatment). The 3D error was calculated and averaged over the successive time period until the next x-ray pair was taken or to the end of the fraction. This value was compared with the 3D error for the same period, without updating the correspondence model. This procedure was applied to a few special cases: for two fractions where a time trend was present, in one or more directions the relation between internal and external signal gradually changed over time, and for three fractions without such a time trend (Fig. 10). The treatment error reduced when the time between two subsequent images was shorter, but if the time period was very small (e.g., 5 s). On the other hand, in some cases, local irregularities could disturb a proper prediction that lasts a longer time, especially if the updating frequency was more or less equal to the breathing frequency or to a multiple of the breathing

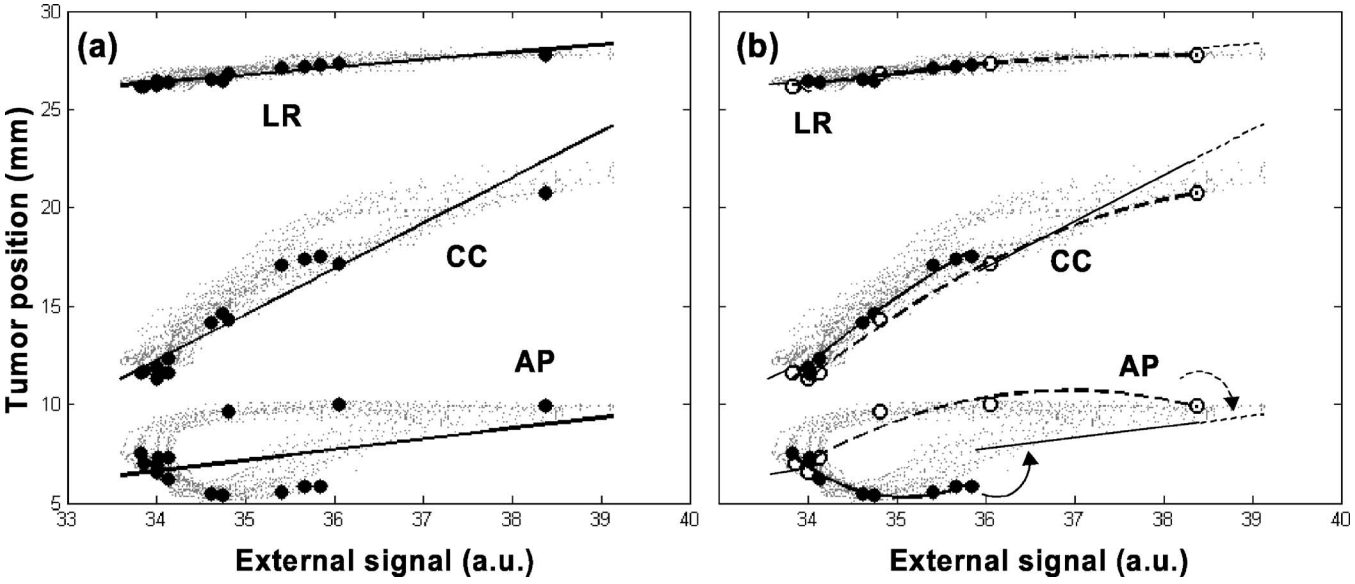

FIG. 4. Linear (a) and polynomial (b) correspondence models for a patient with hysteresis between the internal and external signals, based on 15 simulated x-ray images (solid circles), taken in the first 15 s of the treatment. The actual tumor position as a function of the external signal is plotted as an illustration in the background (tiny dots). For the polynomial model, two polynomials are fitted through the data, one for the inhale phase (continuous line, solid circles) and one for the exhale phase (dashed line, open circles). The polynomial model is only valid in the range of the x-ray images (otherwise large extrapolation errors can occur). In case the external signal exceeds this range, the prediction switches back to the linear correspondence model (see arrows in the AP example).

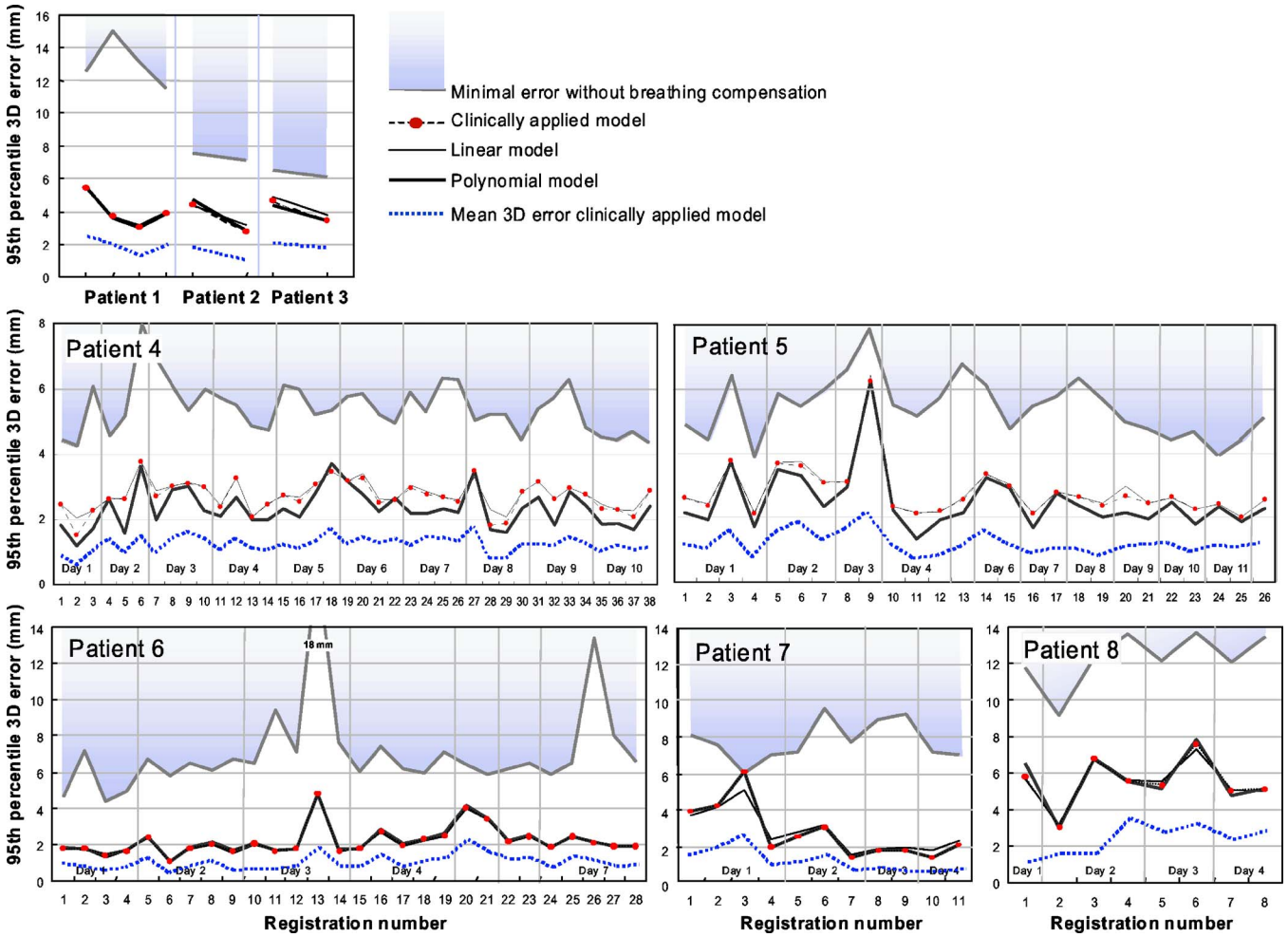

FIG. 5. The 95th percentile of the residual 3D treatment error for both the linear and polynomial models, and for the clinically applied protocol (choice between linear and polynomial model for each direction separately) for all beams of patients 1–8. The treatment error will be (much) smaller than this value for 95% of the time. For the noncompensated treatment error, the minimum value is calculated; set-up errors should be added for a more realistic representation (grey area).

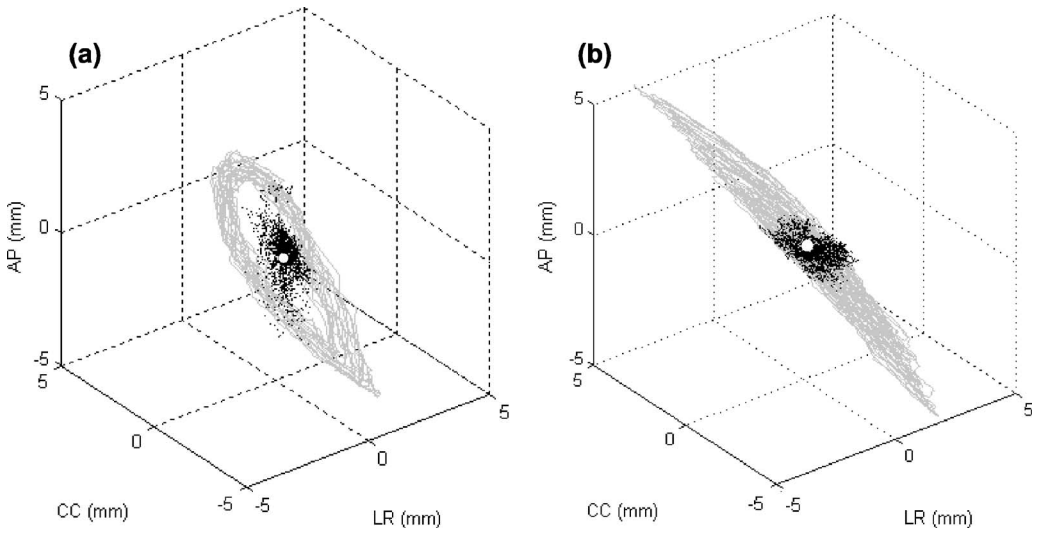

FIG. 6. (a) 3D representation of the treatment error for a noncompensated irradiation (continuous line) and breathing compensated treatment (dots) for the same patient as shown in Fig. 4 (pattern 1, polynomial model). The white dot represents the predicted tumor position. In case of the noncompensated treatment, the tumor is never in this position, while for the breathing compensated treatment the tumor is much closer to this position most of the time. (b) The same as (a), now for the patient without hysteresis (Fig. 3), the residual error is much smaller in the breathing compensated case, all models gave similar results.

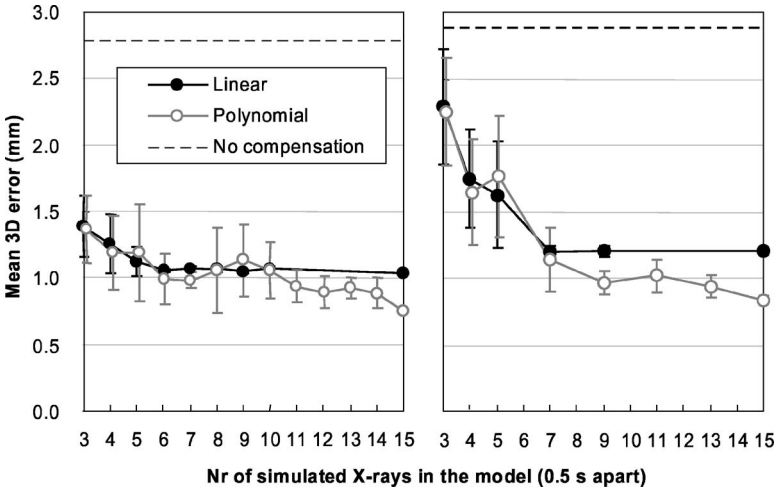

FIG. 7. Residual treatment error (3D) as a function of the number of simulated x-ray images in the correspondence model (patient 4 and 5). For the linear model, 8 or more x-ray images give reliable results, for the polynomial model, at least 15 x-ray images are necessary for a stable prediction of tumor position.

frequency (data not shown). In those cases the breathing cycle will not be sampled homogeneously and thus will lead to inferior prediction models.

Updating the complete model halfway through the fraction resulted in a larger improvement in treatment error than updating one x-ray pair every 15 s. By doing so, changes are apparently better implemented in the model, compared to the other update schemes for which it takes longer before the complete model is updated. However, the overall improvement is less than the improvement obtained with the fastest

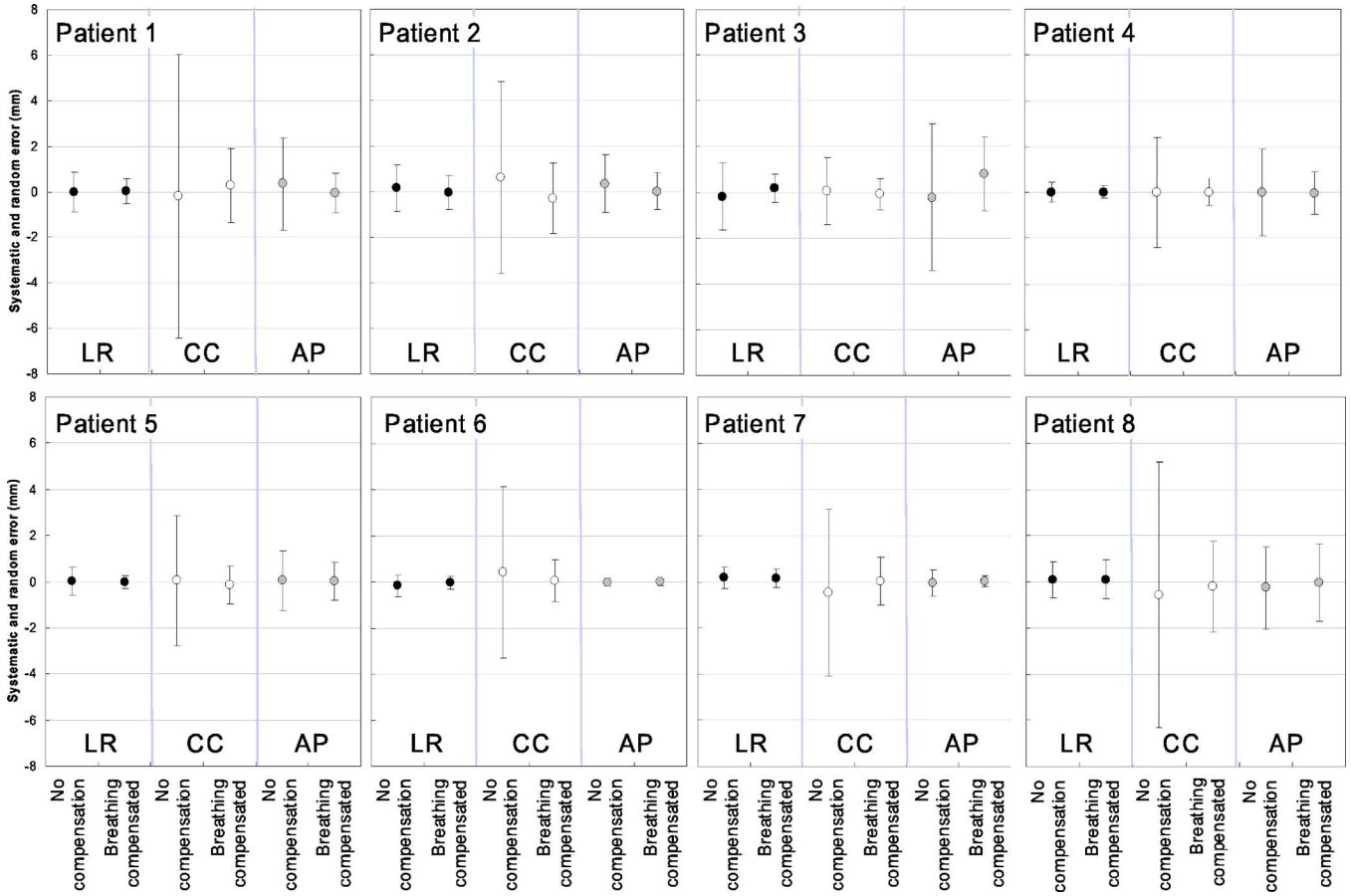

FIG. 8. Overview of systematic and random treatment errors (1SD), averaged for each patient, for the noncompensated case and for the polynomial correspondence model. For the noncompensated case, the "predicted" tumor position is assumed to be the average tumor position during the first 10 s of the treatment; note that patient positioning errors should be added to these values to obtain a realistic estimate.

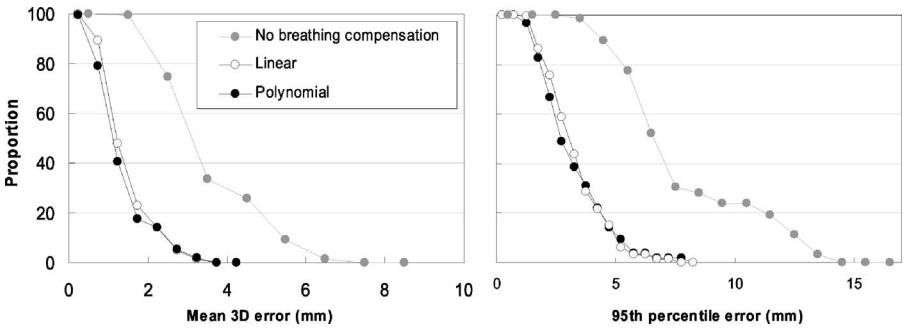

FIG. 9. Histograms of the mean and the 95th percentage 3D treatment error for all patients (weighted average) for the noncompensated treatment, linear and polynomial models.

update frequency (5 s). This is because the faster update frequency leads to earlier (though smaller) adjustments of the model at each step. The earlier a correction is made, the smaller the overall residual error will be.

For the patients without a time trend, the time interval between updating did not make much difference.

B. Hysteresis

The polynomial model performed better for the patients who showed internal hysteresis or had a time delay between the internal and external motion (patients 4 and 5). In case of extreme time delays between internal and external motion, the performance of this model will be reduced because the determination of the inhale and exhale phase is solely based on the external signal. It can happen that the "inhale" polynomial is based on tumor positions that are, in fact, in the exhale phase and the other way around. The amount of hysteresis observed in the studied patients did not result in large errors due to this effect.

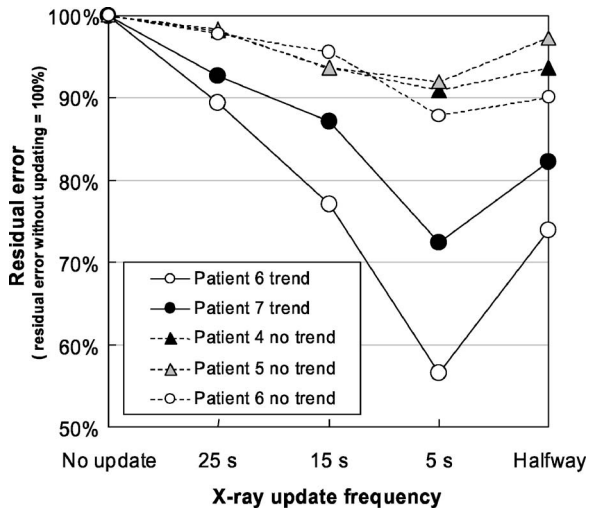

FIG. 10. Effects of the x-ray update frequency for two registrations with a time trend and three without. At different regular time-intervals, an update x-ray was simulated (every 5, 15, 25 s) or a complete update of the model (15 x-ray images at 1 s distance) halfway through the recording. The correspondence model was updated accordingly. The residual 3D error was calculated and averaged. This value was compared with the mean 3D error for the same period, without updating the correspondence model.

IV. DISCUSSION

The reduction in treatment error due to breathing motion, using Synchrony™ RTS with a simple linear model and a limited number of x-ray images, is large, even for patients with irregular breathing and/or internal or external hysteresis (Figs. 5 and 8). Fine-tuning of the correspondence model by using polynomial functions reduced the treatment error by a few more mm for those patients. Hysteresis between internal and external signal was frequently observed and could change from day to day, however, the correspondence models were found to be quite stable during a time period representative for the update frequency of the Synchrony™ RTS (<1–4 min, less than 100 ms for acquiring one frame). Commonly present breathing irregularities as baseline shifts, changes in breathing frequency, and amplitude are usually accounted for by Synchrony™ RTS and do not increase treatment time. As imaging is performed before each treatment session, set-up errors are virtually absent and the relation between internal and external signal is established. Long-term time trends are detected and corrected by updating the model at regular intervals throughout the treatment. Nevertheless, some residual motion will be sustained because of noise in the data (±1 mm), inaccuracy of the models and the system (also ±1 mm), and time trends or sudden changes that are not picked up by the system. These errors should be accounted for by an appropriate margin. The residual motion observed in this study is comparable with the study of Korreman *et al.*[15] in which the authors analyzed the correlation between internal and external motion by fluoroscopy, based on fits through the entire dataset.

Ways of reducing the effect of breathing motion are abdominal compression,[16] active breathing control,[9] gating,[5] tracking,[17] or a combination of these. For all these techniques, the relation between internal tumor motion and the external surrogate is important, but is not always handled in an optimal way. Many of the techniques rely on a constant (one-to-one) relation between internal and external motion without hysteresis and require regular and steady breathing patterns throughout the treatment. Tumor motion is not as regular as often is assumed; changes in motion pattern with both random and systematic components are frequently observed over the course of radiotherapy, as is hysteresis.[10,18–21] The present study is not contradicting this.

With breath-hold techniques additional errors may be induced.[22] Cyberknife's Synchrony™ RTS is the only system that on-line determines *and* deals with the not-always linear relation between internal tumor motion and the external surrogate.

The main requirement for accurate dose delivery with Synchrony™ RTS is absence of significant fiducial marker migration and tumor deformation during radiotherapy. Imura *et al.*[23] reported earlier that the reliability of the marker position lasts for 2–4 weeks from the start of radiotherapy. In contrast to conventional radiation for lung cancer patients consisting of schemes with fractions of 2–2.5 Gy during several weeks, lung cancer patients treated with the Cyberknife receive 3×20 Gy within one week so, in this time frame, marker migration is not likely to occur.

The Synchrony™ RTS, as was used at the time of this study, could only randomly sample the breathing cycle; there was no possibility to sequence the x-ray imaging system such that it covers a whole breathing cycle homogeneously. As tumors tend to spend more time in the exhale phase, the RTS will have an increased probability of missing images of the tumor position at, or close to its inhale position. In that case, the reliability and accuracy of the polynomial fit can be hampered because the range on which the polynomial fit was based will be smaller, making the model more sensitive to noise. Furthermore, the model switches back to the, in some cases less accurate, linear model if the range of the external signal exceeds the range for which the polynomial model is determined.

We found that in this data-set random sampling of the x-ray sequence (pattern 2 and CK) gave rise to a larger variability in the results and a slightly larger 3D error, compared to a series of x-ray images at 0.5 s time intervals for the polynomial model (pattern 1). As expected, the linear model was less sensitive for these effects. This finding underlines that it is important that all phases of the breathing cycle are sufficiently sampled by the imaging system. An automatic x-ray acquisition sequence (i.e., triggered by the external marker signal) that covers one or two breathing cycles would improve the correspondence models. Concerning the frequency of imaging to update the model, a trade-off should be made between excess patient x-ray exposure, accuracy of the model, and also treatment time. For patients with stable correction models, less imaging is necessary. For patients with irregular breathing patterns, faster updating will reduce the treatment error. A decision about an appropriate update frequency can be made based on analysis of the residual errors, reported back by the system during treatment.

Furthermore, the choice of the most appropriate prediction model cannot be made correctly based on a least-square fit using the 15 x-ray images (clinical protocol). This is made clear by Fig. 5 (patients 4 and 5); in almost all cases the polynomial model provided a better prediction in case hysteresis was present, and a similar prediction as the linear model in the other cases. Apparently a least-squares analysis based on 15 x-ray images does not contain enough information to select the best fitting model, particularly not if the breathing cycle is sampled inhomogeneously, which is likely to occur with the current clinical x-ray sequence. The weighting that was applied to favor simpler models does not always result in the choice of the most optimal corresponding error.

With the Cyberknife system, irradiation time is long compared to conventional radiotherapy, a typical treatment lasts for 60–90 min in which a patient is not expected to be totally without movement. Updating the model frequently is therefore essential. Safety interlocks prevent irradiation after the patient, for example, coughs or shows external motion larger than a preset level. After each update x-ray image, the true tumor position is automatically checked against the predicted position and, if the deviation between these two is larger than 3 mm (value applied in our center), the entire model is rebuilt before the treatment can continue.

Delays in positioning the radiation source at the offsets, calculated by the correlation model, necessitates the introduction of a time-prediction mechanism that compensates for these delays. Such a mechanism exists in current implementation of Synchrony and accounts for the 115 ms between computing the real-time offset of the tumor and the ability of the robot to position the radiation source accordingly. By inspecting the patterns of LED movement in the immediate past, the predictor compensates for the delay and predicts the target position 115 ms in the future. The predictor works well for patients with regular breathing pattern and adjusts quickly (with 1–2 s) to changes in breathing pattern. If the breathing pattern is highly irregular, then it is possible that the errors from the predictor can be significant. However, unlike the correlation model where the actual target position information is available only after an image acquisition, the error in prediction is always known 115 ms after the prediction has taken place (predicted value—actual value). This error is displayed on Synchrony's user interface and can be monitored to ensure that the value of prediction error is within acceptable clinical limits.

Because of the high precision, the Cyberknife in combination with Synchrony™ RTS can ideally be used for hyperfractionated treatments, also making up for prolonged treatment times and the inevitable time trends that will be present in the patient.

[a]Author to whom correspondence should be addressed. Telephone: 00-31-10-4391131; Fax: +31.10.4391012. Electronic mail: y.seppenwoolde@erasmusmc.nl

[1]J. R. Adler, Jr., S. D. Chang, M. J. Murphy, J. Doty, P. Geis, and S. L. Hancock, "The Cyberknife: a frameless robotic system for radiosurgery," Stereotact. Funct. Neurosurg. **69**, 124–128 (1997).
[2]S. D. Chang and J. R. Adler, "Robotics and radiosurgery—the cyberknife," Stereotact. Funct. Neurosurg. **76**, 204–208 (2001).
[3]S. D. Chang, W. Main, D. P. Martin, I. C. Gibbs, and M. P. Heilbrun, "An analysis of the accuracy of the CyberKnife: a robotic frameless stereotactic radiosurgical system," Neurosurgery **52**, 140–146 (2003).
[4]A. Schweikard, G. Glosser, M. Bodduluri, M. J. Murphy, and J. R. Adler, "Robotic motion compensation for respiratory movement during radiosurgery," Comput. Aided Surg. **5**, 263–277 (2000).
[5]H. D. Kubo and B. C. Hill, "Respiration gated radiotherapy treatment: a technical study," Phys. Med. Biol. **41**, 83–91 (1996).
[6]H. D. Kubo and L. Wang, "Introduction of audio gating to further reduce organ motion in breathing synchronized radiotherapy," Med. Phys. **29**, 345–350 (2002).
[7]S. Minohara, T. Kanai, M. Endo, K. Noda, and M. Kanazawa, "Respira-

tory gated irradiation system for heavy-ion radiotherapy," Int. J. Radiat. Oncol., Biol., Phys. **47**, 1097–1103 (2000).
[8]L. A. Dawson, C. Eccles, J. P. Bissonnette, and K. K. Brock, "Accuracy of daily image guidance for hypofractionated liver radiotherapy with active breathing control," Int. J. Radiat. Oncol., Biol., Phys. **62**, 1247–1252 (2005).
[9]J. W. Wong, M. B. Sharpe, D. A. Jaffray, V. R. Kini, J. M. Robertson, J. S. Stromberg, and A. A. Martinez, "The use of active breathing control (ABC) to reduce margin for breathing motion," Int. J. Radiat. Oncol., Biol., Phys. **44**, 911–919 (1999).
[10]Y. Seppenwoolde, H. Shirato, K. Kitamura, S. Shimizu, M. van Herk, J. V. Lebesque, and K. Miyasaka, "Precise and real-time measurement of 3D tumor motion in lung due to breathing and heartbeat, measured during radiotherapy," Int. J. Radiat. Oncol., Biol., Phys. **53**, 822–834 (2002).
[11]H. Shirato, S. Shimizu, T. Kunieda, K. Kitamura, M. van Herk, K. Kagei, T. Nishioka, S. Hashimoto, K. Fujita, H. Aoyama, K. Tsuchiya, K. Kudo, and K. Miyasaka, "Physical aspects of a real-time tumor-tracking system for gated radiotherapy," Int. J. Radiat. Oncol., Biol., Phys. **48**, 1187–1195 (2000).
[12]R. I. Berbeco, S. Nishioka, H. Shirato, G. T. Chen, and S. B. Jiang, "Residual motion of lung tumors in gated radiotherapy with external respiratory surrogates," Phys. Med. Biol. **50**, 3655–3667 (2005).
[13]H. Shirato, T. Harada, T. Harabayashi, K. Hida, H. Endo, K. Kitamura, R. Onimaru, K. Yamazaki, N. Kurauchi, T. Shimizu, N. Shinohara, M. Matsushita, H. Dosaka-Akita, and K. Miyasaka, "Feasibility of insertion/implantation of 2.0-mm-diameter gold internal fiducial markers for precise setup and real-time tumor tracking in radiotherapy," Int. J. Radiat. Oncol., Biol., Phys. **56**, 240–247 (2003).
[14]H. Shirato, Y. Seppenwoolde, K. Kitamura, R. Onimura, and S. Shimizu, "Intrafractional tumor motion: Lung and liver," Semin. Radiat. Oncol. **14**, 10–18 (2004).
[15]S. Korreman *et al.*, "Predictability of lung tumor motion based on external markers and nonlinear modelling," Med. Phys. (submitted)/AAPM 2004 abstract (2006).
[16]J. Wulf, U. Hadinger, U. Oppitz, W. Thiele, and M. Flentje, "Impact of target reproducibility on tumor dose in stereotactic radiotherapy of targets in the lung and liver," Radiother. Oncol. **66**, 141–150 (2003).
[17]S. Nill, J. Unkelbach, L. Dietrich, and U. Oelfke, "Online correction for respiratory motion: evaluation of two different imaging geometries," Phys. Med. Biol. **50**, 4087–4096 (2005).
[18]G. Hugo, C. Vargas, J. Liang, L. Kestin, J. W. Wong, and D. Yan, "Changes in the respiratory pattern during radiotherapy for cancer in the lung," Radiother. Oncol. **78**, 326–331 (2006).
[19]Y. Tsunashima, T. Sakae, Y. Shioyama, K. Kagei, T. Terunuma, A. Nohtomi, and Y. Akine, "Correlation between the respiratory waveform measured using a respiratory sensor and 3D tumor motion in gated radiotherapy," Int. J. Radiat. Oncol., Biol., Phys. **60**, 951–958 (2004).
[20]G. K. Prisk, J. Hammer, and C. J. Newth, "Techniques for measurement of thoracoabdominal asynchrony," Pediatr. Pulmonol **34**, 462–472 (2002).
[21]C. Ozhasoglu and M. J. Murphy, "Issues in respiratory motion compensation during external-beam radiotherapy," Int. J. Radiat. Oncol., Biol., Phys. **52**, 1389–1399 (2002).
[22]J. M. Blackall, S. Ahmad, M. E. Miquel, J. R. McClelland, D. B. Landau, and D. J. Hawkes, "MRI-based measurements of respiratory motion variability and assessment of imaging strategies for radiotherapy planning," Phys. Med. Biol. **51**, 4147–4169 (2006).
[23]M. Imura, K. Yamazaki, H. Shirato, R. Onimaru, M. Fujino, S. Shimizu, T. Harada, S. Ogura, H. Dosaka-Akita, K. Miyasaka, and M. Nishimura, "Insertion and fixation of fiducial markers for setup and tracking of lung tumors in radiotherapy," Int. J. Radiat. Oncol., Biol., Phys. **63**, 1442–1447 (2005).